Tailoring PEGylated nanoparticle surface modulates inflammatory response in vascular endothelial cells

Soudeh Tehrani, Jean-Michel Rabanel, Samuel Legeay, Jérôme Cayon, Jérémie Riou, Patrick Saulnier, Sylvie Marleau, V. Gaëlle Roullin, Patrice Hildgen, Guillaume Bastiat

Tailoring PEGylated nanoparticle surface modulates inflammatory response in vascular endothelial cells

Soudeh F. Tehrani[1,2], Jean-Michel Rabanel[3], Samuel Legeay[2], Jérôme Cayon[4], Jérémie Riou[2], Patrick Saulnier[2], Sylvie Marleau[1], V. Gaëlle Roullin[1], Patrice Hildgen[1], Guillaume Bastiat[2,*]

[1] Faculty of Pharmacy, Université de Montréal, C.P. 6128, succursale Centre-ville Montréal (Québec), H3C 3J7, Canada

[2] Univ Angers, Inserm, CNRS, MINT, SFR ICAT, F-49000 Angers, France.

[3] INRS Centre Armand-Frappier Santé Biotechnologie, 531 Boul. des Prairies, Laval (Québec), H7V 1B7, Canada

[4] Univ Angers, Plateforme d'Analyse Cellulaire et Moléculaire (PACeM), SFR ICAT, F-49000 Angers, France.

* Corresponding author. E-mail addresses: guillaume.bastiat@univ-angers.fr

Keywords: PEG-PLA nanoparticle; bEnd.3; HUVEC; cytokine; chemokine; Reactive oxygen species

Abstract

Polymer nanoparticles (NPs) are extensively studied as drug delivery systems for various therapeutic indications, including drug and imaging agent delivery to the brain. Despite intensive research, their toxicological profile has yet to be fully characterized. In particular, the more subtle effects of nanomaterials on inflammatory processes have scarcely been investigated. Surface properties of NPs are amongst parameters governing interactions between living cells and NPs. They could considerably influence the toxicity and inflammatory response of the cells exposed to NPs.

Polymeric NPs investigated here present a core-shell structure. The core is constituted of hydrophobic poly(lactic acid) (PLA) block and the surface is composed of a shell of hydrophilic block of polyethylene glycol (PEG). The effect of PEG chain length coating on the expression of genes involved in the inflammation response was investigated in two vascular endothelial cell lines (bEnd.3 and HUVEC) by qPCR. Moreover, ROS generation following NP uptake was evaluated.

PEGylated NPs induce a mild and transient activation of inflammatory cytokine and chemokine genes. However, differences in PEG chain length did not show any significant effect on cytokine and chemokine gene expression and PEGylated NPs did not trigger ROS generation.

The present results could contribute significantly to a deeper understanding of nanomaterial interactions and toxicity with vascular endothelial cells, guiding scientists in material coating choices.

1. Introduction

Polymer nanoparticles (NPs) are extensively studied for brain delivery strategies of drugs and imaging agents [1-5]. A number of studies have shown that NPs could improve drug efficacy by enhancing brain tissue penetration [6-8]. NPs could also decrease drug toxicity by limiting peripheral side effects. Moreover, NPs developed for the treatment of cancer or chronic brain diseases are generally administered as repeated intravenous injections. Therefore, the potential toxicity of the NP drug delivery system itself should constitute a primary concern during the development of a new nanoformulation. NPs must not induce toxic effects on cells with which they come into direct contact, such as vascular endothelial cells [9], macrophages [10], cells comprising filtration organs [11]. Therefore, in-depth investigation of the NP's effect on the inflammatory response in different cell lines, particularly in vascular endothelial cells (VECs), is crucial. Yet, the inflammation and immune responses of VECs in contact with polymeric NPs are seldom reported and little information on the subject is currently available.

Brain microvascular endothelial cells play a crucial role in the blood-brain barrier (BBB) functions. Due to its selective permeability, the BBB protects the brain against pathogens and other toxic chemicals, thereby maintaining brain homeostasis. The BBB is particularly sensitive to different types of insults by pathogens or foreign materials, inducing inflammatory responses. Inflammation can trigger numerous biological alterations of the endothelium, including secretion of pro-inflammatory mediators [12], up-regulation of adhesion molecules as well as pro-coagulant activity [13]. These endothelial dysfunctions could lead to the modulation of BBB permeability [14,15] which, in turn, may alter brain homeostasis as well as brain disease progression [16].

As any foreign material introduced in the bloodstream, NPs could elicit different biological responses including inflammation. Rational design of NPs can influence their inflammatory properties. It has been reported that NP physicochemical properties such as shape [17], size distribution [18], surface charge [19-21], surface chemical composition [22] and poly(ethylene glycol) (PEG) chain surface density [23] could influence their cytotoxicity level by modulating the inflammatory and immune-inflammatory responses. PEG is a hydrophilic polymer, widely used as surface coating to improve the NPs stability and reduce their premature clearance from the systemic circulation [24]. A few

studies have reported the generation of IgM [25] and hypersensitivity reactions to PEG in patients [26,27].

In a previous study, we established a correlation between surface PEG chain length and the extent of PLA-PEG NP endocytosis and transcytosis across an *in vitro* BBB model [28]. PEG corona affects NP BBB translocation by different mechanisms. First by providing longer time in blood circulation as a consequence of improved resistance to opsonisation, decreased macrophage capture and increased colloidal stability. With an enhanced circulation time, NPs increase their chance to be captured and transported by the BBB into the brain [29,30]. Second, plasma proteins such as Apolipoprotein E (ApoE) could be absorbed on the PEG corona and stimulate BBB translocation by receptor-mediated endocytosis [31]. However, the influence of PEG chain length on cytotoxicity and induction of inflammatory response by PEGylated NPs in VECs remains to be investigated. In this article, the impact of PEG chain length at the PLA NP surface on the cytotoxicity, inflammation response and ROS production on two different VEC models, mouse brain endothelial (bEnd.3) cells and HUVEC, was investigated. PEGylated PLA NPs were designed with various PEG chain lengths from 1 to 10 kDa and covalently tethered to PLA surface. In addition, non-covalent PEG modification of PLA NPs was done using Pluronic® F68, a non-ionic PEGylated surfactant able to adsorb at the surface of PLA NPs, and all the NPs were compared to non-PEGylated PLA NPs. The expression of genes involved in the inflammation upon exposure to PEGylated PLA NPs was investigated by qPCR, and the ROS production was measured in both VEC models using a fluorescence technique. The systematic exploration of the inflammatory response of VECs upon exposure to PEGylated NPs showed that NPs trigger a transient increase in gene expression of inflammatory cytokines and chemokines. However, PEG chain length could not be correlated to the inflammatory response observed.

2. Materials and Methods

2.1. Chemical Materials & Reagents

All chemical and biological reagents are fully described in supplementary information (SI) section.

2.2. Synthesis and characterization of polyethylene glycol-poly(lactic acid) diblock copolymer

PLA-BZ and diblock PLA-PEGX polymers (X: 1, 2, 5 and 10 kDa) were obtained by ring-opening polymerization (ROP) as previously reported [22]. The synthesis and the characterization of polymers used in this study are fully detailed in SI.

2.3. Nanoparticle preparation and characterization

Fluorescent-labeled and non-labeled, PEGylated PLA NPs without any surfactant (Cy5-PLA-PEGX and PLA-PEGX NPs, respectively) were prepared by a nanoprecipitation method with the diblock Cy5-PLA-PEGX and/or PLA-PEGX copolymers (X: 1, 2, 5 and 10 kDa). Non-PEGylated PLA NPs (PLA NPs) were prepared with PLA-BZ polymer. In addition, Fluorescent-labeled and non-labeled, PEGylated PLA NPs with surfactant (Cy5-PLA-F68 and PLA-F68 NPs, respectively) were prepared with Cy5-PLA-BZ and/or PLA-BZ polymer and Pluronic® F68 surfactant. Nanoparticle preparation and characterization including size measurements by dynamic light scattering (DLS) and nanoparticle tracking analysis (NTA) as well as residual endotoxin determination are detailed in SI.

2.4. Cell culture

bEnd.3 cells (ATCC CRL-2299) and HUVEC (Lonza, C2519A) were used within 20 and 4 passages, respectively. bEnd.3 cells were cultured in DMEM supplemented with 10% FBS, 1% (*v/v*) non-essential amino acid solution and 1% antibiotic solution. Cells were maintained at 37 ± 0.5°C under a 5% CO_2 atmosphere. HUVEC were grown on regular culture plates in EGM™ medium supplemented with 10% FBS. Cells were maintained at 37 ± 0.5°C under a 5% CO_2 atmosphere.

2.5. Cytotoxicity Assay

The effect of PLA, PLA-F68 and PLA-PEGX NP exposure on the mitochondrial activity of endothelial cells was assessed on bEnd.3 and HUVEC cells by using the 3-[4,5-dimethylthiazol-2-yl]-3,5-diphenyl tetrazolium bromide (MTT) test. Cells were seeded at a density of 5×10^3 cells/well in 96-well plates. After 24 h, medium was discarded and replaced by 200 µL/well of PLA, PLA-F68 or PLA-PEGX NPs diluted in cell culture medium at concentrations ranging from 12.5 to 1,000 µg/mL (n= 4, *i.e.* four independent assays, each in quadruplicate). Untreated cells were used as negative control, whereas cells exposed to 0.1% (*w/v*) Triton-X-100 were used as positive control. After 24 h, NPs and Triton-X-100 were removed and replaced by fresh medium. Fifty µL of a MTT solution (5 mg/mL) was added to each well and incubated at 37°C for 3 h. After medium aspiration, 200 µL of DMSO were added to each well to solubilize the MTT formazan crystals. Twenty-five µL of 0.1 M glycine buffer solution at pH 10.5 were then added to each well. Absorbance was measured at 570 nm using a CLARIOstar 96-well plate reader (BMG Labtech, Champigny-sur-Marne, France).

2.6. Endocytosis kinetics

bEnd.3 and HUVEC cells were seeded into 6-wells plates at a density of 2×10^4 cells/cm^2. After the cell confluence was reached, medium was replaced by medium containing equivalent number of Cy5-PLA-PEGX NPs with a final concentration of 1.76 10^{10} NPs/mL. After incubation times of 1, 3, 6 and 24 h, cell medium was removed and the cell monolayer was washed twice with PBS. Cells were dissociated by 0.25% trypsin-EDTA phenol red (Thermo Fisher Scientific, Illkirch, France) at 37°C for 5 min. The cell suspensions were centrifuged at 1,000 g for 5 min. The cells were washed twice with PBS, pH 7.4 and finally resuspended in 1% (*w/v*) PFA in PBS. The analyses were performed on a FACScalibur cytometer (Becton-Dickinson, Billerica, MA, USA). The fluorescence of the cells was followed at excitation and emission wavelengths of 650 and 670 nm, respectively.

For imaging, bEnd.3 cells were seeded on glass slides in 24-well plate. After reaching 90% confluence, the cell monolayer was exposed to equivalent number of NPs for each

batch (1.76×10^{10} NPs/mL) for 24 h in complete medium. After washing with PBS, cell nuclei were stained with DAPI and cells were imaged by confocal microscopy using a Leica TCS SP8 AOBS (Leica Microsystems, Wetzlar, Germany).

2.7. Quantitative polymerase chain reaction

The effects of PLA, PLA-F68 and PLA-PEGX NPs on expression of inflammatory cytokines and chemokines were studied on HUVEC and bend.3 cells. First, cells were seeded in T25 flasks and incubated at 5% CO_2, 37°C and 95% humidity. After reaching 80% confluence, cells were treated with 1 mg/mL of PLA, PLA-F68 or PLA-PEGX NPs in culture medium for 6 and 24 h. LPS solutions at 0.2 and 1 µg/mL were used as positive controls and untreated cells as negative control. After incubation, the nanosuspensions were removed and cells were washed twice with PBS. Cells were dissociated by 0.25% trypsin-EDTA phenol red, centrifuged at 1,000 *g* for 5 min and resuspended in PBS. The washing step was repeated twice. Finally, cell pellets were recovered and kept at -80°C until further use.

Total RNA was extracted and purified using RNeasy Microkit (QIAGEN FRANCE SAS, Courtaboeuf, France). Extracted RNA was treated with DNase (10 U DNase I/µg total RNA). RNA concentrations were determined using a ND-2000 NanoDrop (Thermo Fisher Scientific, Illkirch-Graffenstaden, France). Input RNA concentrations were normalized before the reverse transcription step. First strand cDNA synthesis was performed according to the manufacturer's instructions with a SuperScript™ II Reverse Transcriptase (Invitrogen, Villebon-sur-Yvette, France), in combination with random hexamers. Following first-strand cDNA synthesis, cDNAs were purified with Qiaquick PCR purification kit (QIAGEN FRANCE SAS, Courtaboeuf, France) and eluted in 40 µL RNAse free water (Millipore SAS, Molsheim, France). cDNA (3 ng) was mixed with Maxima™ SYBR Green qPCR Master Mix (Thermo Fisher Scientific, Illkirch-Graffenstaden, France) and primer mix (0.3 µM) in a final volume of 10 µL. Amplification was carried out on a LightCycler 480 (Roche Diagnostics, Meylan, France) with a first denaturation step at 95°C for 10 min, followed by 40 cycles of 15 s at 95°C and 30 s at 60°C. A melting curve analysis was performed after amplification to determine the primer specificity for the targeted genes. A mean cycle threshold value

(Cq) was obtained from 2 measurements for each cDNA. Specific gene expression was calculated by using the $2^{-\Delta\Delta CT}$ method [32]. The gene expression of three housekeeping genes, namely glyceraldehyde 3-phosphate dehydrogenase (GAPDH), B2M (β2-Microglobulin) and Beta-actin (ACTB), were applied as reference genes.

2.8. Intracellular reactive oxygen species (ROS) measurement

The effects of PLA, PLA-F68 and PLA-PEGX NP concentrations and exposure time on ROS production were tested on HUVEC and bend.3 cells. Cells were seeded at a density of 1×10^4 cells/well in 96-well microplates and incubated for 24 h at 5% CO_2, 37°C and 95% humidity. Both bEnd.3 and HUVEC cells were grown to approximately 80% confluency and then treated with 200 µL of PLA, PLA-F68 or PLA-PEGX NPs at either 50, 250 and 1,000 µg/mL for 2 and 6 h. LPS at concentrations of 0.2, 0.5 and 1 µg/mL were used as positive controls (exposure time: 2 and 6 h). H_2O_2 (0.03 and 0.3% (*v/v*)) was used as a second positive control to generate a burst of ROS production. The duration of the treatment with H_2O_2 was set at 30 min. After incubation, all media was discarded and cells were washed twice with PBS. They were then incubated with 2′,7′-Dichlorofluorescin diacetate (DCFH-DA) in medium (20 µM) for 30 min and washed 3 times with PBS. Sample fluorescence was assessed at excitation and emission wavelengths of 485 and 530 nm, respectively, using a CLARIOstar 96-well plate reader (BMG Labtech, Champigny-sur-Marne, France).

Sample fluorescence was normalized to cell protein content assessed by Bradford protein assay on lysed cells. Briefly, the cells were lysed with 50µL of 0.2 M NaOH and at 37°C for 30 min. Two-hundred µL of Bradford reagent were plated in 96-well plates and then 10 µL of lysed cells were added to each well. A calibration curve was established by using a series of Bovine Serum Albumin (BSA) as protein standards in the 10.9 - 700 µg/mL range. The absorbance of 96-well plates was assessed at 595 nm on a CLARIOstar 96-well plate reader (BMG Labtech, Champigny-sur-Marne, France). ROS relative levels were calculated as follows:

$$\text{ROS relative level} = \frac{\text{Normalized treated cells fluorescence}}{\text{Normalized untreated cells fluorescence}}$$

2.9. Statistical analysis

Statistical analysis of cytotoxicity data: the normality of data distribution was confirmed by Q-Q plots, and the hypothesis of homoscedasticity between variances of all groups was not rejected using the Levene's test (p-value = 0.043). Then, the parametric ANOVA 1F test was performed between all the groups, followed by a post-hoc Dunnett's test for pairwise comparisons. Differences were considered significant for p-value lower than 0.05.

Statistical test for ROS data: the normality of data distribution was not confirmed by Q-Q plots. Then the non-parametric Kruskal–Wallis test was performed between all the groups, followed by a post-hoc Dunn's test for pairwise comparisons. Differences were considered significant for p-value lower than 0.05.

Statistical analysis for qPCR data: the non-parametric Kruskal–Wallis test was performed between all the groups as a function of PEG chain lengths, followed by a post-hoc Dunn's test for pairwise comparisons. The non-parametric Mann-Whitney U test was performed between the groups at 6 and 24 h. Differences were considered significant for p-value lower than 0.05.

The analyses were not blinded.

3. Results

3.1. Nanoparticle preparation and characterization

PLA-PEGX NPs were formed from PLA-PEGX copolymers (X: 1, 2, 5 and 10 kDa) (**Table S1**) displaying a PEG content of less than 15% (*w/w*). Adjusting the PEG weight content to less than 15% (*w/w*) yielded solid NPs with similar mechanical properties, as well as comparable colloidal stability in biological environments [33]. Indeed, it was previously shown that a PEG content greater than 20% (*w/w*) led to the formation of polymeric nanoaggregates rather than solid NPs [33,34]. These PEGylated PLA NPs were designed without surfactant, and for comparison, we also formed PLA NPs using non PEGylated PLA polymer with and without Pluronic® F68, a PEGylated surfactant, *i.e.* PLA-F68 NPs and PLA NPs, respectively.

NP size distributions were assessed by DLS and NTA. Whatever the PLA-PEGX copolymers used for the NP design, the size distributions of PLA-PEGX NPs determined by DLS were similar, with Z-average values of ~ 100 nm and polydispersity (PdI) values lower than 0.2, corresponding to a monomodal and monodisperse size distribution. It is in line with the characterization obtained by NTA with a mean hydrodynamic diameter of ~ 100 nm, with a dispersion of ~ 25 nm (**Table 1**). To check the endocytosis profiles of the NPS, fluorescent-labelled, PEGylated NPs were designed (Cy5-PLA-PEGX NPs). The same size distributions were obtained (**Table S2** and **Figure S1**). Size distributions obtained for PLA NPs and PLA-F68 NPs were slightly different with higher values for hydrodynamic diameter: Z-average values of ~ 135 and 120 nm, with PdI values close or higher than 0.2. This slight increase in size was also observed by NTA (**Table 1**, **Table S2** and **Figure S1**). In addition, PEG chain surface densities were kept constant: ~ 0.2 chain/nm^2 (**Table 1**) (0.1 chain/nm^2 for PLA-F68 NPs). In this study, in order to assess the influence of PEG chain length on inflammatory processes, we considered these characteristics as constant and only the PEG chain lengths vary for these NPs. Only the Zeta potential value of the NP decreased with increased PEG chain length, which has been previously correlated with enhanced PEG shielding [35].

Prior incubation with vascular endothelial cell, nanosuspensions were tested for their endotoxin content by end-point chromogenic Limulus Amebocyte Lysate (LAL) test. Endotoxin contamination is a common issue in nanomedicine development and it is critical for the interpretation of nanotoxicity and transcriptional response to nanomaterial exposure [36]. The endotoxin content for all stock nanosuspensions was less than the FDA recommended limits for injectable drugs, *i.e.* 0.5 EU/mL or approximately 0.1-0.2 ng/mL [37]. PLA-F68 NPs was making exception with an endotoxin level slightly above the limit (**Table S3**). This level, though, is not considered sufficient to elicit a transcriptional response by vascular endothelial cells as it could be seen in this study, as no transcription inflammatory response was detected upon Pluronic® F68-coated NP exposure (see section 3.4).

3.2. Cytotoxicity Assay

The impact of PEG chain length at the PLA NP surface on the cytotoxicity, inflammation response and ROS production was studied using bEnd.3 cells and HUVEC. bEnd.3 is an immortalized mouse brain endothelial cell line extensively used as *in vitro* blood-brain barrier models [38], while HUVEC is a primary human cell used as vascular endothelial human model [39]. The cell viability of bEnd.3 cells and HUVEC upon exposure to PLA, PLA-F68 and PLA-PEGX NPs (X: 1, 2, 5 and 10 kDa) was determined after a 24-h incubation time. The NP concentration tested were ranging from 12.5 to 1000 µg/mL Cell viability of bEnd.3 cells measured after 24-h exposure to PLA and PLA-PEG1k NPs significantly decreased (~ 80% of mitochondrial activity) compared to untreated cells over the entire studied concentration range (**Figure 1A** and **Figure S2**). However, no significant effects on the viability were observed after exposing bEnd.3 cells to PLA-F68 and PLA-PEG2k, PLA-PEG5k and PLA-PEG10k NPs

In a similar manner, incubation of HUVEC with PLA-PEGX NPs with X > 1kDa did not elicit any mitochondrial injuries as assessed by the MTT assay, even at the highest NP concentration (1,000 µg/mL) tested. However, mitochondrial injuries of HUVEC slightly but significantly increased for cells treated with PLA, PLA-F68 and PLA-PEG1k NPs at concentrations higher than 500 µg/mL, yet viability remained above 80%. (**Figure 1B** and **Figure S3**). According to the International Organization for Standardization (ISO), if the cell viability remains above 70%, the material is considered non-toxic [40]. As cell viabilities did not decrease below 80%, even for the highest NPs concentrations for the two cell lines, NPs concentrations were set at 1,000 µg/mL, *i.e.* at a sub-toxic concentration, in the subsequent experiments.

No difference in cell morphology between different treatment regimens for the two cells lines was observed (data not shown). It can be interpreted as a lack of PEG length deleterious effect on cell membranes as seen by Soudeh *et al.* for bEnd.3 [28]. It may also suggest that the effect on inflammatory markers expression is not due to general toxicity issues and NP-induced cell apoptosis.

3.3. Endocytosis kinetic

In the NP uptake study, equivalent number of fluorescent-labelled NPs based on NTA measurement (**Table S2**) was added to bEnd.3 cells or HUVEC grown in 6-well plates. Fluorescence signals for all NP batches (for equivalent number of particles) were in a ± 15% interval, except for PLA-PEG1k NPs (**Table S2**). This latter batch showed a total fluorescence signal which is twice as high as that of the other batches. Therefore direct comparison of uptake level between PLA-PEG 1kD NPs and the other NPs batches should take this difference in account.

NP endocytosis kinetic in bEnd.3 cells, as recorded by flow cytometry showed a rapid uptake of NPs followed by a plateau (**Figure 2A**). This plateau corresponds to a steady state equilibrium between NPs endocytosis and exocytosis. No significant differences were found between 6- and 24-h incubation times for PLA-PEG2k, PLA-PEG5k and PLA-PEG10k NPs (**Figure 2A** and **Figure S4**). PLA-PEG5k NPs were endocytosed faster and were more stored in bEnd.3 than other covalently PEGylated NPs as shown previously [28,41]. PLA-F68 NPs were making exception with very high rate of endocytosis compared to all the covalently PEGylated NPs (**Figure 2A**). Confocal images of bEnd.3 cells at 24 h showed internalized NPs in discrete vesicles (**Figure 2C**), and confirmed the higher rate of endocytosis for PLA-F68 NPs. NPs did not appear to be either associated with the membrane or dispersed in the cytoplasm. No differences in intracellular localization for all the NP batches could be evidenced. Similar uptake results were obtained with HUVECs (**Figure 2B & S5**). No significant differences could be observed between 6- and 24-h incubation time except for PLA-PEG1k NPs (**Figure 2B**).

3.4 Quantitative polymerase chain reaction

To delineate the effect of PEG chain length of PLA-PEGX NPs (X: 1, 2, 5 and 10 kDa) on the inflammatory response in bEnd.3 cells and HUVEC, we assessed the relative gene expression of 24 inflammatory cytokines and chemokines by qPCR after 6- or 24-h incubation. Responses to PLA-F68 NPs, wherein Pluronic® F68 is a surfactant widely used in nanoformulations, were evaluated in a similar manner.

Among the 24 cytokines and chemokines tested, mRNA for 10 and 13 pro-inflammatory cytokines and chemokines were detected in bEnd.3 cells (**Table S4**) and HUVECs (**Table**

S5), respectively. Main functions of selected cytokines and chemokines investigated in this study are summarized in **Table S6**.

3.4.1 Gene expression in bEnd.3 cells

The RQ of mRNA expression levels of IL-6, CXCL1, CXCL10, CXCL11, CCL2, ICAM1 and M-CSF in PLA-F68 NPs-treated bEnd.3 cells for 6 and 24 h, were lower than 2 (**Figure 3**), *i.e.* below the detection threshold and therefore could not be considered as biologically significant. A 2-fold change is considered to be the minimum for a biological response to be considered as significant in qPCR analysis [42].

A similar pattern was observed for the expression of IL-6 and CXCL1 relative levels in bEnd.3 cells (**Figure 3A** and **Figure 3B**). bEnd.3 cells, incubated for 6 and 24 h with PLA-PEG1k, displayed a non-significant level of IL-6 and CXCL1 gene expression. On the other hand, the relative mRNA expressions of IL-6 and CXCL1 transiently increased following treatment with PLA-PEGX NPs for 6 h for PEG chain lengths greater than 2 kDa, but they returned to non-significant levels after 24 h. Moreover, no statistically significant difference of mRNA expression level of IL-6 and CXCL1 was observed between PLA-PEGX NPs of different PEG chain lengths. In contrast, IL-6 and CXCL1 mRNA levels were significantly elevated in LPS-induced bEnd.3 cells after 6 h and still remained elevated after 24 h, however at a lower level (**Figure 3A** and **Figure 3B**).

After a 6-h incubation, CXCL10, CCL2 and ICAM-1 gene expressions in bEnd.3 cells treated with PEGylated NPs revealed a significant level of these genes compared to untreated cells (**Figure 3C**, **Figure 3D** and **Figure 3E**). Additionally, in LPS-treated bEnd.3 cells, relative levels of mRNA for CXCL10, CCL2 and ICAM-1 were transiently elevated. At 24 h, levels of CXCL10 mRNA remained elevated in bEnd.3 cells treated with PEGylated NPs, with the exception of PLA-PEG10k. However, CCL2 and ICAM-1 gene expressions did not reach significant levels at 24 h.

Relative levels of CXCL11 (**Figure 3F**) expression for cells treated with PEGylated NPs for 6 h were non-significantly altered for PEG chain lengths shorter than 10 kDa. Additionally, while CXCL11 expression levels detected in bEnd.3 cells treated with LPS were 200- to 400-fold that of untreated cells at 6 h, this increase was short-lived and was found to be undetectable at 24 h.

M-CSF mRNA relative levels after 6-h exposure to PEGylated NPs were 8- to 14-fold higher than untreated cells and remained elevated by 2- to 6-fold at 24 h. In a similar manner, M-CSF gene expression levels in LPS-treated cells were elevated at both 6 and 24 h (**Figure 3G**).

TIMP-1, NF-κB1 and NF-κB3 gene expression did not change significantly at either 6 or 24 h for PEGylated PLA NP- or LPS-treated bEnd.3 cells (**Figure S6**).

3.4.2 Gene expression in HUVEC

The relative expression of IL-6, IL-1α, IL-1β, CXCL1, CXCL10, CXCL11, CCL2, NF-κB1 genes in HUVECs treated with PLA-F68 NPs at 6 and 24 h did not increase significantly compared to untreated cells (**Figure 4**).

The relative mRNA expression levels of three interleukins (IL-6, IL-1α, IL-1β) and CXCL1 chemokine significantly increased for cells treated with PEGylated NPs at 6 h, for PEG lengths higher than or equal to 5 kDa, but decreased to non-significant levels at 24 h. In contrast, the relative mRNA levels of the three interleukins and CXCL1 were significantly enhanced at 6 and 24 h in LPS-induced HUVECs (**Figure 4A** to **Figure 4D**).

CXCL10 and CCL2 mRNA expression levels were significantly increased after 6-h exposure to LPS and PEGylated NPs with PEG lengths higher than 1 kDa (**Figure 4E** and **Figure 4F**). After 24 h, the level of CXCL10 expression dropped significantly but still remained significantly elevated for NPs with PEG lengths greater than 2 kDa and for LPS-treated cells, while significantly high levels of CCL2 mRNA expression endured for LPS-treated cells only.

HUVEC cells, after 6-h incubation with PEGylated NPs, expressed significant levels of CXCL11, particularly for PEG chain lengths higher than 5 kDa (**Figure 4G**). Unexpectedly, this level significantly increased after 24 h. Interestingly, a similar CXCL11 expression pattern was observed for HUVECs treated with LPS 0.2 µg/mL. On the other hand, cells treated with LPS 1 µg/mL did not show a significant difference in CXCL11 expression levels between 6- and 24-h exposure.

NF-κB1 mRNA expression after 6-h incubation with PEGylated NPs or LPS significantly increased, but decreased after 24 h to a non-significant level (**Figure 4H**).

The mRNA expressions of IL-12, M-CSF, ICAM1, TIMP-1, and NF-κB3 in HUVECs, incubated with either PEGylated PLA NPs or LPS, were found below the detection threshold of qPCR (**Figure S7**).

The comparison between the relative expression of inflammatory cytokines and chemokines in bEnd.3 cells and HUVECs showed a general overlap in terms of pattern and timing of gene expression (**Figure S8**).

3.5 Intracellular reactive oxygen species (ROS) measurement

The evolution of ROS levels over time was estimated by quantifying ROS production at 2 and 6 h following cell exposure to the PEGylated PLA NPs. Since ROS are short-lived chemical species, a short incubation time was chosen (2 h). A second time point at 6 h was selected, as relatively high levels of gene expression for inflammatory cytokines and chemokines were detected upon NP and LPS exposure at this time point (**Figure 3** and **Figure 4**). The relative ROS levels in bEnd.3 cells and HUVEC treated with the highest concentration of NPs (1,000 µg/mL) are shown in **Figure 5**. The relative ROS level in cells treated with low (250 µg/mL) and medium (500 µg/mL) concentrations of NPs are shown in **Figure S9**.

The ROS relative levels in bEnd.3 cells treated for 2 and 6 h did not significantly increase with any of the tested PEGylated PLA NPs. The same result was found for PLA and PLA-F68 NPs (**Figure 5A** and **Figure 5B**). Moreover, no significant difference was found between ROS production levels in bEnd.3 cells treated with either low, medium or high concentrations of PLA, PLA-F68 and PLA-PEGX NP suspensions (**Figure S9A/B**). The ROS relative levels in bEnd.3 cells treated for 2 and 6 h with LPS, used as a positive control, increased significantly. Neither a dose-response relationship nor an effect of exposure time was observed in ROS production. However, the ROS generation in LPS-treated bEnd.3 cells significantly increased only for LPS concentrations higher than 0.2 µg/mL at 2 and 6 h (**Figure 5A** and **Figure 5B**).

A similar pattern in the generation of ROS was observed with HUVEC. While the relative ROS production in cells treated with PLA, PLA-F68 and PLA-PEGX NPs did not increase at these time points, cells treated with LPS for 2 and 6 h exhibited significantly increased ROS levels (**Figure 5C**, **Figure 5D** and **Figure S9C/D**). H_2O_2,

used as a positive control, generated higher levels of ROS than LPS and thus PLA, PLA-F68 or PEGylated PLA NPs in both bEnd.3 cells and HUVECs in a concentration-dependent manner (**Figure 5**). The ROS levels induced by H_2O_2 treatment were ~7- and ~14-fold higher than for PEGylated NPs, with H_2O_2 concentrations of 0.03 and 0.3% (*v/v*), respectively.

4. Discussion

In this study, exposure to PLA-PEGX NPs induced a short-lived mild acute inflammatory response in VEC cell lines. However, these observations were independent of PEG chain length, as assessed by the relative mRNA expression levels of various inflammatory cytokines and chemokines. LPS treatment was used as positive control. Non-significant differences in expression of inflammatory genes were generally observed between cells treated with PEGylated NPs or LPS at 6-h. At 24-h however, expression levels generally stayed significantly higher for LPS-treated cells compared to cells treated with PEGylated NPs. In addition, PLA-PEGX NPs did not induce ROS generation despite triggering a certain gene expression level of inflammatory cytokines and chemokines. The very low level of residual endotoxin in nanosuspensions (**Table S3**) rules out a contribution of contaminants on the inflammatory response.

A selected set of inflammatory cytokines and chemokines, as well as adhesion molecules and transcription factors **(Table S4** and **S5)** were thoroughly investigated in response to exposure to polymeric NPs. Three groups of NPs were tested: PLA-PEGX NPs with PEG chain coating covalently attached to NP surface (X between 1 and 10 kDa); pure PLA NPs (PLA) and PLA NPs with PEG chains (Pluronic® F68) adsorbed onto the NP surface (PLA-F68 NPs). PLA NPs were used as control to clarify the influence of the PEG coating on the induction of inflammation. However, PLA NPs demonstrated low colloidal stability, rapidly precipitating in culture medium [28]. The separation of PLA NP aggregates from cells was not technically feasible. Thus, the PLA NPs were excluded from qPCR analyses. The expression levels of inflammatory cytokine and chemokine mRNA in bEnd.3 cells and HUVEC in contact with PLA NPs were not evaluated. To further investigate the influence of PEG coating, pure PLA NPs were thus prepared with Pluronic® F68, a non-ionic surfactant stabilizing particles by adsorption at their surface.

Pluronic® F68 is a triblock copolymer which contains two chains of 3 kDa-PEG attached to a central block of poly (propylene glycol), widely used in nanoformulation. In contrast to PEGylated NPs in which the PEG chains are covalently attached to the NPs, in PLA-F68 NPs, Pluronic® F68 is strongly physisorbed onto the PLA core and forms a dynamic corona on the surface of the NPs. Therefore, there is an equilibrium between Pluronic® F68 adsorbed on the surface of the NPs and Pluronic® F68 remaining in the bulk solution [43]. PLA-F68 PEG density at equilibrium state is lower than PEG chain densities found for PLA-PEGX NPs (**Table 1**).

4.1 Interleukin gene expression

A similar pattern of interleukin gene expression in response to either LPS or NPs was observed in HUVEC and bEnd.3 cells, except that HUVEC expressed IL-6, IL-1α and IL-1β while bEnd.3 cells expressed only IL-6. This difference was not surprising as mRNA expression levels of cytokines in response to the same inflammatory agent can vary among different cell types [44].

Secretion of IL-6, IL-1α and IL-1β plays a key role in acute inflammatory responses [45]. Transient IL-1α, IL-1β and IL-6 mRNA expression enhancement in both cell lines implies that an acute inflammation response was induced by PLA-PEGX NPs. One of the rare study evaluating the inflammatory properties of polymeric NPs showed that secretion of IL-6 by HUVEC was not enhanced upon contact with poly[acrylonitrile-co-(N-vinylpyrrolidone)] NPs after 72-h exposure [46]. However, a longer exposure time may not be optimal to detect IL-6 gene expression, as it is usually associated with acute phase events. In contrast to PEGylated NPs, inorganic NPs induced IL-6 and IL-1β gene expression in HUVECs, which may be still significantly elevated after 24 h [47,48]. In the current study, the pattern of IL-1α, IL-1β and IL-6 gene expression following contact with inorganic NPs is closer to the expression pattern generated in LPS-treated cells than those in PLA-PEGX NP treated cells (**Figure 3A** and **Figure 4A/B/C**). The mRNA expression levels suggest that LPS induced an acute inflammatory response associated with elevated expression of cytokines even after 24 h. In agreement, the inflammatory response triggered by LPS *via* the Toll-like receptor 4 is long-lasting compared to that of PLA-PEGX NPs [49].

4.2. Tumor necrosis factor α and colony stimulating factor expression

Tumor Necrosis Factor α (TNFα) is one of the most important cytokines, promoting the expression of many other cytokines and chemokines [50-52]. The expression of TNFα mRNA in LPS-induced HUVEC was found to be maximal after 1-h stimulation and decreased sharply after 2 h, to reach undetectable levels at 6 h [53]. Due to this early gene expression response, as expected, the mRNA levels of TNFα were not observed either at 6 or 24 h in our studies (data not shown)**.** No conclusion could therefore be drawn regarding the possible induction of TNFα by PEGylated polymeric NPs.

Macrophage–Colony Stimulating Factor (M-CSF) is a cytokine which regulates monocyte survival and maturation and mediates the differentiation of monocytes into macrophages [54]. PLA-PEGX NPs significantly increased the expression of M-CSF in bEnd.3 cells at 6 and 24 h. Interestingly PLA-PEGX NPs induced the same gene expression pattern as LPS in bEnd.3 cells (**Figure 3G**).

4.3. Inflammatory chemokines

Non-activated endothelial cells do not secrete pro-inflammatory chemokines. Therefore, the increase in the mRNA level of chemokines is an indicator of the triggered inflammatory response [55]. Moreover, cytokines and chemokines are often generated in a cascade: the expression of two or more cytokines or chemokines can synergistically stimulate the expression of other cytokines and chemokines [52]. For instance, IL-6 secretion was observed to upregulate CXCL1 expression in brain endothelial cells [56]. Consistent with an acute inflammatory response, the expression of CXCL1 in HUVEC and bEnd.3 cells transiently increased after 6-h exposure to PLA-PEGX NPs (**Figure 3B** and **4D**). Unlike TiO_2 NPs, PLA-PEGX NPs produced a shorter-term expression of CXCL1. Indeed, the expression of CXCL1 in brain endothelial cells in contact with TiO_2 NPs is much more pronounced (300-fold *versus* untreated cells) after 24 h and it remained high even after five days [57].

CXCL10 and CXCL11 mRNA expression levels increased, thus constituting an indicator of the inflammatory response [58,59]. Actually, CXCL10 and CXCL11 induce recruitment and activation of neutrophils and adhesion of T-cells to endothelial cells,

respectively [60]. However, CXCL10 and CXCL11 gene expressions in VECs, in response to an exposure to polymeric NPs, have not yet been explored. CXCL10 and CXCL11 mRNA levels remained high upon cell exposure to PLA-PEGX NPs after 24 h (**Figure 3C/F** and **Figure 4E/G**). This finding suggests that PLA-PEGX NPs could potentially induce a longer-lasting inflammatory response, involving immune cell recruitment.

PEGylated PLA NPs induced the gene expression of monocyte chemoattractant chemokine CCL2 in bEnd.3 cells and HUVEC at 6 h (**Figure 3D** and **Figure 4F**). Our results suggested that PLA-PEGX NPs may initiate monocyte recruitment and adhesion to activated endothelial cells [48]. PEGylated gold NPs, with sizes similar to our NPs, did not significantly increase CCL2 secretion in HUVEC at short (4 h) or medium-term incubation times (24 or 72 h) [61]. This difference could be explained by different NP doses (150 µg/mL *versus* 1,000 µg/mL), or by the mechanical properties of NP core due to core deformability, affecting PEGylated NP uptake rate in VECs [62]. The duration of CCL2 gene expression induction by PLA-PEGX NPs was shorter than its induction with highly inflammatory NPs, such as silica or TiO_2 NPs. The latter showed significantly higher CCL2 expression levels, even after 24 h, compared to controls [48,57].

4.4. Adhesion molecule

Intercellular adhesion molecule 1 (ICAM1) is an adhesion molecule whose main role is to mediate the adhesion of leukocytes to endothelial cells in an acute or chronic inflammatory situation [63]. ICAM1 gene expression in bEnd.3 cells significantly increased in the presence of PLA-PEGX NPs (**Figure 3E**). However, its gene expression levels in HUVEC were not significantly modified upon NP exposure (**Figure S7C**). This was not surprising as even highly inflammatory NPs such as Co_3O_4 and TiO_2 NPs only induced a modest increase (2-fold) of gene expression levels in treated HUVEC [64]. On the other hand, PEGylated gold NPs did not significantly increase the secretion of ICAM1 from HUVEC following short (4 h) or medium incubation periods (24 or 72 h) [61].

4.5. Transcription factor: NF-κB

NF-κB is a pleiotropic transcription factor playing a pivotal role in controlling gene expression of cytokines such as TNF-α, IL-1α, IL-1β and IL-6, chemokines such as CCL2, CXCL1 and CXCL10, and adhesion molecules including ICAM1. Its action is triggered by different cues, including LPS through Toll-like receptors [65]. PLA-PEGX NPs significantly upregulated NF-κB1 gene expression in HUVEC (**Figure 4H**), but not in bEnd.3 cells (**Figure S6B**). This difference could be related to the cell origin (human umbilical *versus* mouse brain) and cell type (immortalized *versus* primary cells). Interestingly, the expression of IL-1α, IL-1β and NF-κB1 increased simultaneously only in HUVEC. Thus, it is hypothesized that NF-κB1 could participate in upregulating the gene encoding IL-1α and IL-1β.

4.6. Covalent *versus* physisorbed PEG-coated NPs

Cytokine and chemokine gene expressions did not significantly increase upon exposure to PLA-F68 NPs, contrary to exposure to PLA-PEGX NPs (**Figure 3** and **Figure 4**). This result supports the harmlessness of residual endotoxin level in this NP preparation (**Table S3**). This behavioral difference could be related to differences in PEG chain surface density (**Table 1**) and in the nature of chemical interactions between PEG chains and NP cores. Our results contrasted with a previous study reporting an increased secretion of CCL2 and IL-6 after a 24-h exposure of epithelial cells to PLGA-F68 NPs [66]. This disparity could stem from differences in cell type used in the assays and the fact that supplementary regulations could take place at the protein translation step. Interestingly, this study also showed that free Pluronic® F68 did not increase CCL2 and IL-6 secretions [66]. This last result emphasizes the significant role of the nature of the PEG chain chemical bonding (free molecules, physisorbed or covalently tethered to a NP core) can play in inducing inflammatory responses.

4.7. ROS generation by NP exposure

ROS generation and inflammation processes are tightly linked and there is a mutual relation between their induction, wherein ROS can induce cytokine production and pro-inflammatory cytokines tend to increase ROS levels [67]. Inflammation induced by metal

NPs has been linked to ROS generation at the NP surface or through metal ion release [68,69]. However, the information regarding relation between inflammation and ROS generation by polymer NPs is scarce. Recently, positively-coated, PLGA-based NPs were found to increase ROS generation [70]. In our case, all tested NPs failed to significantly increase ROS generation (**Figure 5**). These results are in line with those obtained by Yu *et al.* showing that a PEG coating added on the surface of iron oxide NPs decreased ROS generation compared to bare iron oxide NPs [71]. Contrary to PEGylated NPs, LPS exposure generated a significant level of ROS in both bEnd.3 and HUVEC, as previously reported [72,73]. LPS can generate ROS by cytokine-dependent and cytokine-independent mechanisms. In cytokine-dependent mechanisms, LPS triggers the NF-κB signaling pathway which induces the expression of pro-inflammatory cytokines [73], stimulating ROS production via the NADH oxidase [74]. Cytokine expressions upon PLA-PEGX NPs or LPS exposures were not significantly different in bEnd.3 cells and HUVECs. It can therefore be hypothesized that, during LPS exposure, ROS were mainly generated *via* a cytokine-independent pathway whereas PEGylated NPs are not able to induce ROS production through this pathway.

4.8. Inflammation induction mechanism by polymeric NPs

The mechanisms by which polymeric NPs might induce these responses are currently unexplored. Carbon NPs were shown to act through the direct interactions of NPs with Toll-like receptors to induce inflammatory responses [75]. The roles of carbon NP surface and size on inflammation promotion have been highlighted in epithelial pulmonary cells [76]. Krüger *et al.* showed that inhibiting endocytic pathways decreased the inflammatory response induced by TiO_2 NPs in Caco-2 cells [77]. These results supported the notion that the NPs endocytosis rate could play an important role in the induction of an inflammatory response. The inflammatory response upon contact with PLA-PEGX NPs became significant for longer PEG chains (**Figure 3** and **4**). This result is in agreement with our previous study showing an increased NP endocytosis rate with increasing PEG chain length [28,41] and the present endocytosis kinetic results (**Figure 2**). Overall, these results suggest that the inflammation response triggered by PEGylated NPs occurs intracellularly.

Three parameters could be considered regarding the effect of NP uptake kinetics on transcriptional effects: 1) the entry rate, 2) the level of NP intracellular accumulation at different time points, and finally 3) the final level of intracellular accumulation. Regarding the first point, PLA-PEG5k and PLA-PEG10k NPs are the fastest in both cell lines but it does not translate in specific effects when compared to PLA-PEG2k NPs for instance. Regarding the second point, NPs accumulation reached a plateau, after 6 h, when equilibrium occurs between endocytosis and exocytosis [41]. No significant differences in NP uptake at 6 and 24 h were observed for PLA-PEG2k, PLA-PEG5k and PLA-PEG10k NPs in bend.3 cells and HUVEC (**Figure 2**). Between these two time points inflammatory response tends to fade with time. Therefore, uptake kinetic of NPs was not playing a role in transcriptional differences observed at 6 and 24 h for both cells. It was observed distinct pattern of endocytosis between bEnd.3 cells and HUVEC (**Figure 2**). In both cells, PLA-F68 NPs are more endocytosed than others PLA-PEGX NPs. Loosely bound F68 coating at the surface of polyester NPs had been shown to favor particle entry into cells [78]. NP localization inside the cells could play a role too. NPs dispersed in the cytoplasm, in perinuclear or nuclear localization could be expected to interact more directly with the cell machinery than NPs sequestered in endosomes as they appeared in bEnd.3 microscopy images at 24 h (**Figure 2C**).

In vivo, inflammation events in response to NPs are the result of a complex interplay of different cell lineages. VECs are only one element of the puzzle. Interestingly, Liu *et al.* demonstrated that the production of inflammatory cytokines and chemokines induced by silica NPs was significantly higher in a co-culture model of monocyte and endothelial cells than in a HUVEC monoculture model [79]. Notwithstanding what is currently known of the central role played by endothelial cells in the inflammatory response to NPs, exploring the interactions between endothelial and immune cells is key to achieving a deeper understanding of the inflammatory and immune responses to PEGylated NPs *in vivo*.

5. Conclusion

The inflammatory response to polymeric NPs is an underexplored topic. This study intended to fill the knowledge gap relative to PEGylated polymer NPs inflammation-

mediated nanotoxicity. Overall, the lesson learnt from this systematic exploration of the inflammatory response of VECs upon exposure to PEGylated NPs was that NPs trigger a transient increase in gene expression of some important inflammatory cytokines and chemokines. While PEG chain length could not be correlated to the inflammatory response observed, PEG chain attachment (tethered or physisorbed) was shown to significantly modulate cytokine and chemokine production. The effects of longer exposures as well as accumulation of polymeric NPs in VECs still remain to be explored to obtain a more complete representation of the inflammatory response to polymeric NPs. Likewise, the interactions of VECs with immune cells upon PEGylated NP exposure *in vivo* warrant further investigation.

Supporting Information

1) Chemical Materials & Reagents, 2) Synthesis and characterization of polyethylene glycol-poly (lactic acid) diblock copolymer, 3) Nanoparticle preparation and characterizations, 4) Endotoxin level determination, 5) Cytotoxicity assays, 6) Nanoparticle uptake kinetic by bEnd.3 cells: flow cytometry histograms; 7) Nanoparticle uptake kinetic by HUVEC: flow cytometry histograms; 8) Quantitative polymerase chain reaction of inflammatory cytokines and chemokines; 9) Comparison of gene expression pattern between bEnd.3 cells and HUVEC; and 10) Intracellular reactive oxygen species (ROS) quantifications, can be found in Supporting Information.

Acknowledgments

S.F.T thanks « Mitacs-Globalink Research Award » and « Programme de bourses pour de courts séjours d'études universitaires à l'extérieur du Québec» from the Ministry of Education and Higher Education of Québec (MEES) and the Faculty of Pharmacy of the Université de Montréal for travel award. P.H. acknowledges support by NSERC. JMR thanks the NSERC/CRSNG postdoctoral grant program for financial support. This study was partially supported by a « Fonds de Recherche du Québec, Nature et Technologies » grant (FRQ-NT, Government of Québec, Canada; grant # 191486) and by the « Fondation ARC pour la Recherche sur le Cancer » (France).

Declaration of interest

The authors declared no conflict of interest.

References

[1] S. Nie, Understanding and overcoming major barriers in cancer nanomedicine, Nanomedicine, 5 (2010) 523-528.

[2] Y. Zhou, Z. Peng, E.S. Seven, R.M. Leblanc, Crossing the blood-brain barrier with nanoparticles, Journal of Controlled Release, 270 (2018) 290-303.

[3] J.M. Rabanel, M. Perrotte, C. Ramassamy, Nanotechnology at the Rescue of Neurodegenerative Diseases: Tools for Early Diagnostic, in: M. Rai, A. Yadav (Eds.), Nanobiotechnology in Neurodegenerative Diseases, Springer International Publishing, Denmark, 2019, pp. 19-48.

[4] G. Tosi, J.T. Duskey, J. Kreuter, Nanoparticles as carriers for drug delivery of macromolecules across the blood-brain barrier, Expert Opinion on Drug Delivery, 17 (2020) 23-32.

[5] Z. Weisen, A. Mehta, Z. Tong, L. Esser, N.H. Voelcker, Development of Polymeric Nanoparticles for Blood-Brain Barrier Transfer-Strategies and Challenges, Advanced Science, 8 (2021) 2003937.

[6] S. Wohlfart, S. Gelperina, J. Kreuter, Transport of drugs across the blood–brain barrier by nanoparticles, Journal of Controlled Release, 161 (2012) 264-273.

[7] C. Saraiva, C. Praça, R. Ferreira, T. Santos, L. Ferreira, L. Bernardino, Nanoparticle-mediated brain drug delivery: Overcoming blood–brain barrier to treat neurodegenerative diseases, Journal of Controlled Release, 235 (2016) 34-47.

[8] F.C. Lam, S.W. Morton, J. Wyckoff, T.L. Vu Han, M.K. Hwang, A. Maffa, E. Balkanska-Sinclair, M.B. Yaffe, S.R. Floyd, P.T. Hammond, Enhanced efficacy of combined temozolomide and bromodomain inhibitor therapy for gliomas using targeted nanoparticles, Nature Communication, 9 (2018) 1991.

[9] S.K. Murthy, Nanoparticles in modern medicine: state of the art and future challenges, International journal of nanomedicine, 2 (2007) 129-141.

[10] D. Ling, T. Hyeon, Chemical Design of Biocompatible Iron Oxide Nanoparticles for Medical Applications, Small, 9 (2013) 1450-1466.

[11] H.H. Gustafson, D. Holt-Casper, D.W. Grainger, H. Ghandehari, Nanoparticle Uptake: The Phagocyte Problem, Nano today, 10 (2015) 487-510.

[12] W.J. Trickler, S.M. Lantz, R.C. Murdock, A.M. Schrand, B.L. Robinson, G.D. Newport, J.J. Schlager, S.J. Oldenburg, M.G. Paule, J.W. Slikker, S.M. Hussain, S.F. Ali,

Silver Nanoparticle Induced Blood-Brain Barrier Inflammation and Increased Permeability in Primary Rat Brain Microvessel Endothelial Cells, Toxicological Sciences, 118 (2010) 160-170.

[13] J.-B. Dietrich, The adhesion molecule ICAM-1 and its regulation in relation with the blood–brain barrier, Journal of Neuroimmunology, 128 (2002) 58-68.

[14] N.J. Abbott, Inflammatory Mediators and Modulation of Blood–Brain Barrier Permeability, Cellular and Molecular Neurobiology, 20 (2000) 131-147.

[15] M. Charabati, J.M. Rabanel, C. Ramassamy, A. Prat, Overcoming the Brain Barriers: From Immune Cells to Nanoparticles, Trends in pharmacological sciences, 41 (2020) 42-54.

[16] M.D. Sweeney, A.P. Sagare, B.V. Zlokovic, Blood–brain barrier breakdown in Alzheimer disease and other neurodegenerative disorders, Nature Reviews Neurology, 14 (2018) 133.

[17] B. Zhang, P. Sai Lung, S. Zhao, Z. Chu, W. Chrzanowski, Q. Li, Shape dependent cytotoxicity of PLGA-PEG nanoparticles on human cells, Scientific Reports, 7 (2017) 7315.

[18] H.J. Yen, S.H. Hsu, C.L. Tsai, Cytotoxicity and immunological response of gold and silver nanoparticles of different sizes, Small, 5 (2009) 1553-1561.

[19] Y. Tan, S. Li, B.R. Pitt, L. Huang, The inhibitory role of CpG immunostimulatory motifs in cationic lipid vector-mediated transgene expression in vivo, Human gene therapy, 10 (1999) 2153-2161.

[20] R. Kedmi, N. Ben-Arie, D. Peer, The systemic toxicity of positively charged lipid nanoparticles and the role of Toll-like receptor 4 in immune activation, Biomaterials, 31 (2010) 6867-6875.

[21] J.-M. Rabanel, V. Adibnia, S.F. Tehrani, S. Sanche, P. Hildgen, X. Banquy, C. Ramassamy, Nanoparticle heterogeneity: an emerging structural parameter influencing particle fate in biological media?, Nanoscale, 11 (2019) 383-406.

[22] J.P. Ryman-Rasmussen, J.E. Riviere, N.A. Monteiro-Riviere, Surface coatings determine cytotoxicity and irritation potential of quantum dot nanoparticles in epidermal keratinocytes, The Journal of investigative dermatology, 127 (2007) 143-153.

[23] N. Bertrand, P. Grenier, M. Mahmoudi, E.M. Lima, E.A. Appel, F. Dormont, J.-M. Lim, R. Karnik, R. Langer, O.C. Farokhzad, Mechanistic understanding of in vivo protein corona formation on polymeric nanoparticles and impact on pharmacokinetics, Nature communications, 8 (2017) 777.

[24] Z. Amoozgar, Y. Yeo, Recent advances in stealth coating of nanoparticle drug delivery systems, Wiley Interdisciplinary Reviews: Nanomedicine and Nanobiotechnology, 4 (2012) 219-233.

[25] P. Grenier, I.M. de Oliveira Viana, E.M. Lima, N. Bertrand, Anti-polyethylene glycol antibodies alter the protein corona deposited on nanoparticles and the physiological pathways regulating their fate in vivo, Journal of controlled release, 287 (2018) 121-131.

[26] E. Wenande, L.H. Garvey, Immediate-type hypersensitivity to polyethylene glycols: a review, Clinical and experimental allergy : journal of the British Society for Allergy and Clinical Immunology, 46 (2016) 907-922.

[27] J. de Vrieze, Suspicions grow that nanoparticles in Pfizer's COVID-19 vaccine trigger rare allergic reactions, Science, (2020).

[28] S.F. Tehrani, F. Bernard-Patrzynski, I. Puscas, G. Leclair, P. Hildgen, V.G. Roullin, Length of surface PEG modulates nanocarrier transcytosis across brain vascular endothelial cells, Nanomedicine: Nanotechnology, Biology and Medicine, 16 (2019) 185-194.

[29] P. Calvo, B. Gouritin, H. Chacun, D. Desmaële, J. D'Angelo, J.P. Noel, D. Georgin, E. Fattal, J.P. Andreux, P. Couvreur, Long-circulating PEGylated polycyanoacrylate nanoparticles as new drug carrier for brain delivery, Pharmaceutical Research, 18 (2001) 1157-1166.

[30] J.M. Rabanel, P. Hildgen, X. Banquy, Assessment of PEG on polymeric particles surface, a key step in drug carrier translation, Journal of Controlled Release, 185 (2014) 71-87.

[31] H.R. Kim, K. Andrieux, S. Gil, M. Taverna, H. Chacun, D. Desmaële, F. Taran, D. Georgin, P. Couvreur, Translocation of Poly(ethylene glycol-co-hexadecyl)cyanoacrylate Nanoparticles into Rat Brain Endothelial Cells: Role of Apolipoproteins in Receptor-Mediated Endocytosis, Biomacromolecules, 8 (2007) 793-799.

[32] J. Vandesompele, K. De Preter, F. Pattyn, B. Poppe, N. Van Roy, A. De Paepe, F. Speleman, Accurate normalization of real-time quantitative RT-PCR data by geometric averaging of multiple internal control genes, Genome Biology, 3 (2002) research0034.0031.

[33] J.-M. Rabanel, J. Faivre, S.F. Tehrani, A. Lalloz, P. Hildgen, X. Banquy, Effect of the Polymer Architecture on the Structural and Biophysical Properties of PEG–PLA Nanoparticles, ACS applied materials & interfaces, 7 (2015) 10374-10385.

[34] T. Riley, S. Stolnik, C.R. Heald, C.D. Xiong, M.C. Garnett, L. Illum, S.S. Davis, S.C. Purkiss, R.J. Barlow, P.R. Gellert, Physicochemical Evaluation of Nanoparticles

Assembled from Poly(lactic acid)−Poly(ethylene glycol) (PLA−PEG) Block Copolymers as Drug Delivery Vehicles, Langmuir, 17 (2001) 3168-3174.

[35] R. Gref, M. Lück, P. Quellec, M. Marchand, E. Dellacherie, S. Harnisch, T. Blunk, R.H. Müller, 'Stealth' corona-core nanoparticles surface modified by polyethylene glycol (PEG): influences of the corona (PEG chain length and surface density) and of the core composition on phagocytic uptake and plasma protein adsorption, Colloids and surfaces. B, Biointerfaces, 18 (2000) 301-313.

[36] Y. Li, D. Boraschi, Endotoxin contamination: a key element in the interpretation of nanosafety studies, Nanomedicine, 11 (2016) 269-287.

[37] U.S. Pharmacopea, General Chapters, General Tests & Assays (85) Bacterial endotoxin test, in, 2011.

[38] R.C. Brown, A.P. Morris, R.G. O'Neil, Tight junction protein expression and barrier properties of immortalized mouse brain microvessel endothelial cells, Brain Research, 1130 (2007) 17-30.

[39] D. Onat, D. Brillon, P.C. Colombo, A.M. Schmidt, Human vascular endothelial cells: a model system for studying vascular inflammation in diabetes and atherosclerosis, Current diabetes reports, 11 (2011) 193-202.

[40] I.-B. International Organization for Standardization, Biological evaluation of medical devices–Part 5: Tests for in vitro cytotoxicity, in, International Organization for Standardization Geneve, Switzerland, 2009.

[41] J.-M. Rabanel, P.-A. Piec, S. Landri, S.A. Patten, C. Ramassamy, Transport of PEGylated-PLA nanoparticles across a blood brain barrier model, entry into neuronal cells and in vivo brain bioavailability, Journal of Controlled Release, 328 (2020) 679-695.

[42] R.C. Edmunds, J.K. McIntyre, J.A. Luckenbach, D.H. Baldwin, J.P. Incardona, Toward enhanced MIQE compliance: reference residual normalization of qPCR gene expression data, Journal of biomolecular techniques : JBT, 25 (2014) 54-60.

[43] O. Al-Hanbali, K.J. Rutt, D.K. Sarker, A.C. Hunter, S.M. Moghimi, Concentration dependent structural ordering of poloxamine 908 on polystyrene nanoparticles and their modulatory role on complement consumption, Journal of nanoscience and nanotechnology, 6 (2006) 3126-3133.

[44] S.S. Mano, K. Kanehira, S. Sonezaki, A. Taniguchi, Effect of polyethylene glycol modification of TiO(2)nanoparticles on cytotoxicity and gene expressions in human cell lines, International journal of molecular sciences, 13 (2012) 3703-3717.

[45] J.-M. Zhang, J. An, Cytokines, inflammation, and pain, International anesthesiology clinics, 45 (2007) 27-37.

[46] C. Wischke, A. Krüger, T. Roch, B.F. Pierce, W. Li, F. Jung, A. Lendlein, Endothelial cell response to (co)polymer nanoparticles depending on the inflammatory environment and comonomer ratio, European Journal of Pharmaceutics and Biopharmaceutics, 84 (2013) 288-296.

[47] J.J. Corbalan, C. Medina, A. Jacoby, T. Malinski, M. Radomski, Amorphous silica nanoparticles trigger nitric oxide/peroxynitrite imbalance in human endothelial cells: Inflammatory and cytotoxic effects, 2011.

[48] C. Guo, Y. Xia, P. Niu, L. Jiang, J. Duan, Y. Yu, X. Zhou, Y. Li, Z. Sun, Silica nanoparticles induce oxidative stress, inflammation, and endothelial dysfunction in vitro via activation of the MAPK/Nrf2 pathway and nuclear factor-kappaB signaling, International journal of nanomedicine, 10 (2015) 1463-1477.

[49] W. Wang, M. Deng, X. Liu, W. Ai, Q. Tang, J. Hu, TLR4 activation induces nontolerant inflammatory response in endothelial cells, Inflammation, 34 (2011) 509-518.

[50] N.A. Turner, R.S. Mughal, P. Warburton, D.J. O'Regan, S.G. Ball, K.E. Porter, Mechanism of TNFα-induced IL-1α, IL-1β and IL-6 expression in human cardiac fibroblasts: Effects of statins and thiazolidinediones, Cardiovascular Research, 76 (2007) 81-90.

[51] H. Lo, T. Lai, C. Li, W. Wu, TNF-α induces CXCL1 chemokine expression and release in human vascular endothelial cells in vitro via two distinct signaling pathways, Acta pharmacologica Sinica, 35 (2014) 339-350.

[52] A.H. Sprague, R.A. Khalil, Inflammatory cytokines in vascular dysfunction and vascular disease, Biochemical pharmacology, 78 (2009) 539-552.

[53] T. Imaizumi, H. Itaya, K. Fujita, D. Kudoh, S. Kudoh, K. Mori, K. Fujimoto, T. Matsumiya, H. Yoshida, K. Satoh, Expression of tumor necrosis factor-alpha in cultured human endothelial cells stimulated with lipopolysaccharide or interleukin-1alpha, Arteriosclerosis, thrombosis, and vascular biology, 20 (2000) 410-415.

[54] M. Green, M.A. Harrington, A comparison of macrophage colony-stimulating factor (M-CSF) gene expression in primary and immortalized endothelial cells, Journal of hematotherapy & stem cell research, 9 (2000) 237-246.

[55] C.L. Speyer, P.A. Ward, Role of endothelial chemokines and their receptors during inflammation, Journal of investigative surgery : the official journal of the Academy of Surgical Research, 24 (2011) 18-27.

[56] M. Roy, J.-F. Richard, A. Dumas, L. Vallières, CXCL1 can be regulated by IL-6 and promotes granulocyte adhesion to brain capillaries during bacterial toxin exposure and encephalomyelitis, Journal of Neuroinflammation, 9 (2012) 18.

[57] E. Brun, M. Carrière, A. Mabondzo, In vitro evidence of dysregulation of blood–brain barrier function after acute and repeated/long-term exposure to TiO2 nanoparticles, Biomaterials, 33 (2012) 886-896.

[58] E.W. Sorensen, J. Lian, A.J. Ozga, Y. Miyabe, S.W. Ji, S.K. Bromley, T.R. Mempel, A.D. Luster, CXCL10 stabilizes T cell-brain endothelial cell adhesion leading to the induction of cerebral malaria, JCI insight, 3 (2018) e98911.

[59] T. Loos, L. Dekeyzer, S. Struyf, E. Schutyser, K. Gijsbers, M. Gouwy, A. Fraeyman, W. Put, I. Ronsse, B. Grillet, G. Opdenakker, J.V. Damme, P. Proost, TLR ligands and cytokines induce CXCR3 ligands in endothelial cells: enhanced CXCL9 in autoimmune arthritis, Laboratory Investigation, 86 (2006) 902.

[60] J.W. Griffith, C.L. Sokol, A.D. Luster, Chemokines and chemokine receptors: positioning cells for host defense and immunity, Annual review of immunology, 32 (2014) 659-702.

[61] L. Anspach, R.E. Unger, C. Brochhausen, M.I. Gibson, H.A. Klok, C.J. Kirkpatrick, C. Freese, Impact of polymer-modified gold nanoparticles on brain endothelial cells: exclusion of endoplasmic reticulum stress as a potential risk factor, Nanotoxicology, 10 (2016) 1341-1350.

[62] X. Banquy, F. Suarez, A. Argaw, J.-M. Rabanel, P. Grutter, J.-F. Bouchard, P. Hildgen, S. Giasson, Effect of mechanical properties of hydrogel nanoparticles on macrophage cell uptake, Soft Matter, 5 (2009) 3984-3991.

[63] M. Sans, J. Panés, E. Ardite, J.I. Elizalde, Y. Arce, M. Elena, A. Palacín, J.C. Fernández–Checa, D.C. Anderson, R. Lobb, J.M. Piqué, VCAM-1 and ICAM-1 mediate leukocyte-endothelial cell adhesion in rat experimental colitis, Gastroenterology, 116 (1999) 874-883.

[64] R. Alinovi, M. Goldoni, S. Pinelli, M. Campanini, I. Aliatis, D. Bersani, P.P. Lottici, S. Iavicoli, M. Petyx, P. Mozzoni, A. Mutti, Oxidative and pro-inflammatory effects of cobalt and titanium oxide nanoparticles on aortic and venous endothelial cells, Toxicology in vitro : an international journal published in association with BIBRA, 29 (2015) 426-437.

[65] A. Oeckinghaus, S. Ghosh, The NF-kappaB family of transcription factors and its regulation, Cold Spring Harbor perspectives in biology, 1 (2009) a000034-a000034.

[66] N. Grabowski, H. Hillaireau, J. Vergnaud, L.A. Santiago, S. Kerdine-Romer, M. Pallardy, N. Tsapis, E. Fattal, Toxicity of surface-modified PLGA nanoparticles toward lung alveolar epithelial cells, International Journal of Pharmaceutics, 454 (2013) 686-694.

[67] S.K. Biswas, Does the interdependence between oxidative stress and inflammation explain the antioxidant paradox?, Oxidative medicine and cellular longevity, 2016 (2016).

[68] A. Manke, L. Wang, Y. Rojanasakul, Mechanisms of nanoparticle-induced oxidative stress and toxicity, BioMed research international, 2013 (2013) 942916-942916.

[69] P. Khanna, C. Ong, B. Bay, G. Baeg, Nanotoxicity: an interplay of oxidative stress, inflammation and cell death, Nanomaterials, 5 (2015) 1163-1180.

[70] A. Platel, R. Carpentier, E. Becart, G. Mordacq, D. Betbeder, F. Nesslany, Influence of the surface charge of PLGA nanoparticles on their in vitro genotoxicity, cytotoxicity, ROS production and endocytosis, Journal of Applied Toxicology, 36 (2016) 434-444.

[71] M. Yu, S. Huang, K.J. Yu, A.M. Clyne, Dextran and polymer polyethylene glycol (PEG) coating reduce both 5 and 30 nm iron oxide nanoparticle cytotoxicity in 2D and 3D cell culture, International journal of molecular sciences, 13 (2012) 5554-5570.

[72] S.M. Seok, J.M. Kim, T.Y. Park, E.J. Baik, S.H. Lee, Fructose-1,6-bisphosphate ameliorates lipopolysaccharide-induced dysfunction of blood-brain barrier, Archives of pharmacal research, 36 (2013) 1149-1159.

[73] F. Simon, R. Fernández, Early lipopolysaccharide-induced reactive oxygen species production evokes necrotic cell death in human umbilical vein endothelial cells, Journal of hypertension, 27 (2009) 1202-1216.

[74] T. Matsubara, M. Ziff, Increased superoxide anion release from human endothelial cells in response to cytokines, The Journal of Immunology, 137 (1986) 3295-3298.

[75] M. Turabekova, B. Rasulev, M. Theodore, J. Jackman, D. Leszczynska, J. Leszczynski, Immunotoxicity of nanoparticles: a computational study suggests that CNTs and C60 fullerenes might be recognized as pathogens by Toll-like receptors, Nanoscale, 6 (2014) 3488-3495.

[76] C. Monteiller, L. Tran, W. MacNee, S. Faux, A. Jones, B. Miller, K. Donaldson, The pro-inflammatory effects of low-toxicity low-solubility particles, nanoparticles and fine particles, on epithelial cells in vitro: the role of surface area, Occupational and environmental medicine, 64 (2007) 609-615.

[77] K. Krüger, K. Schrader, M. Klempt, Cellular Response to Titanium Dioxide Nanoparticles in Intestinal Epithelial Caco-2 Cells is Dependent on Endocytosis-Associated Structures and Mediated by EGFR, Nanomaterials (Basel, Switzerland), 7 (2017) 79.

[78] L. Mei, Y. Zhang, Y. Zheng, G. Tian, C. Song, D. Yang, H. Chen, H. Sun, Y. Tian, K. Liu, Z. Li, L. Huang, A Novel Docetaxel-Loaded Poly (ε-Caprolactone)/Pluronic F68 Nanoparticle Overcoming Multidrug Resistance for Breast Cancer Treatment, Nanoscale research letters, 4 (2009) 1530-1539.

[79] X. Liu, Y. Xue, T. Ding, J. Sun, Enhancement of proinflammatory and procoagulant responses to silica particles by monocyte-endothelial cell interactions, Particle and Fibre Toxicology, 9(2012) 36.

Table 1. PEGylated PLA NPs characteristics after complete purification (mean ± SD for the data with 3 independent batches and 3 measurements per batch, except for NTA data with 1 batch and 3 measurements).

#	DLS		NTA		Zeta potential (mV)	PEG density* (chain/nm^2)
	Z-ave (nm)	PdI	Mean (nm)	SD (nm)		
PLA NPs	136 ± 2	0.25 ± 0.10	ND	ND	-30 ± 1	NA
PLA-F68 NPs	120 ± 2	0.19 ± 0.07	115	29	-24 ± 1	0.10 ± 0.01
PLA-PEG1k NPs	104 ± 2	0.13 ± 0.02	99	25	-22 ± 2	0.18 ± 0.02
PLA-PEG2k NPs	106 ± 1	0.17 ± 0.01	96	23	-15 ± 2	0.20 ± 0.03
PLA-PEG5k NPs	109 ± 1	0.14 ± 0.01	97	26	-12 ± <1	0.18 ± 0.02
PLA-PEG10k NPs	108 ± 2	0.11 ± 0.02	93	20	-10 ± 1	0.19 ± 0.01

Z-ave : Z-average; PdI: Polydispersity index.
NA: Not Applicable; ND: Not Determined.
* For PEG surface density calculations, please refer to SI

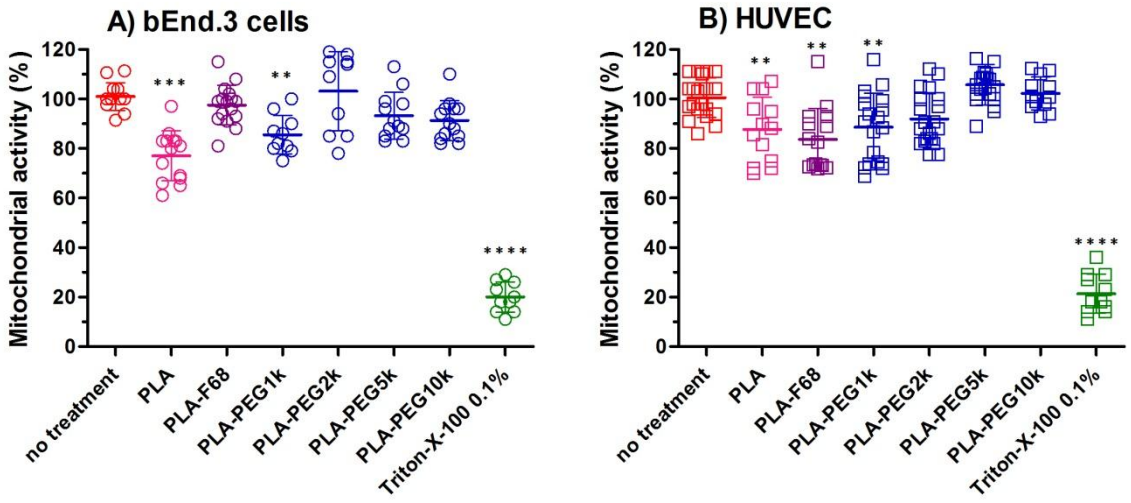

Figure 1. Vascular endothelial cell viability. Cell viability of bEnd.3 cells (A) and HUVEC (B) after a 24-h exposure to PLA (○/□), PLA-F68 (○/□) and PLA-PEGX NPs (X from 1 to 10 kDa) (○/□), at 1,000 µg/mL, *versus* untreated cells (○/□). Triton-X-100 at 0.1% (*w/v*) was used as positive controls (○/□) (n = 4 independent assays and quadruplicate wells per sample per assay; mean ± SD; ** $p < 0.01$, *** $p < 0.001$ and **** $p < 0.0001$ represent the difference significance in cell viability compared to untreated cells).

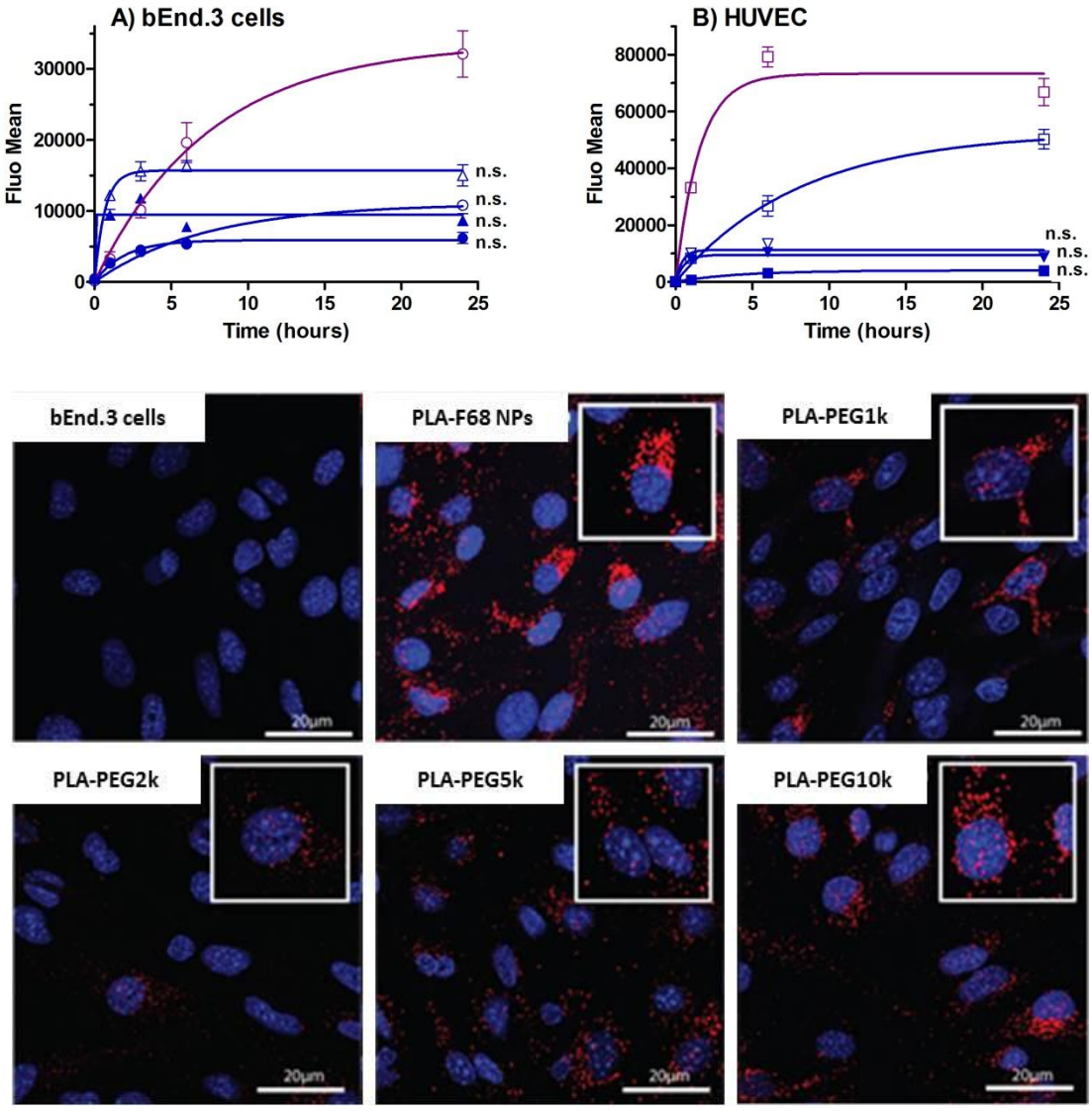

Figure 2. NP endocytosis kinetic in vascular endothelial cells. Uptake kinetic by flow cytometry analysis of bEnd.3 cells (A) and HUVEC (B) after exposure with equivalent number of particles for each NP batch: PLA-F68 (○/□) and PLA-PEGX NPs (blue symbols) with X = 1 (○/□), 2 (●/■), 5 (△/▽) and 10 kDa (▲/▼). Incubations times were set at 1, 3, 6 and 24 h. (C) Confocal images of bEnd.3 cells at 24 h after exposition with NPs. In blue: DAPI staining of cell nuclei, in red: Cy5-labelled NPs. Inserts: confocal images, 4X enlargement of area of interest. Fluorescence mean values were normalized for differences in fluorescent level of NP batches. n.s.: non-significant difference of fluorescence signals between 6- and 24-h incubation times.

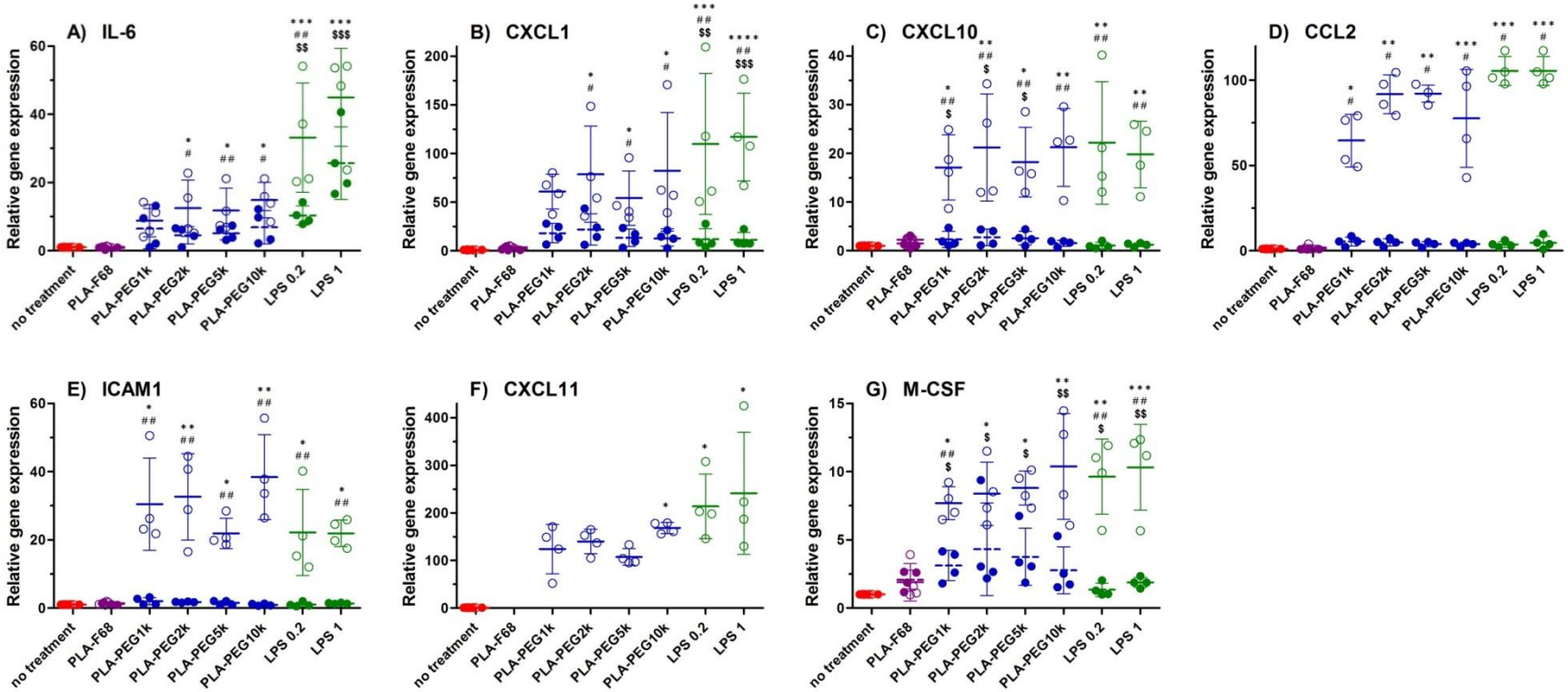

Figure 3. Relative mRNA expression inflammatory for cytokines and chemokines in bEnd.3 cells. A) IL-6, B) CXCL1, C) CXCL10, D) CCL2, E) ICAM1, F) CXCL11 and G) M-CSF, in bEnd.3 cells treated with PLA-F68 (○/●) and PLA-PEGX NPs (X from 1 to 10 kDa) (○/●) for 6 (○/○/○/○) and 24 h (●/●/●/●), at 1,000 µg/mL, *versus* untreated cells (○/●). Two LPS concentrations (0.2 and 1 µg/mL) were used as positive controls (○/●) (n = 4 independent samples; mean ± SD; ∗ $p < 0.05$, ∗∗ $p < 0.01$, ∗∗∗ $p < 0.001$ and ∗∗∗∗ $p < 0.0001$ represent the difference significance in the relative gene expression compared to untreated cells, at 6 h; $ $p < 0.05$, $$ $p < 0.01$ and $$$ $p < 0.001$ represent the difference significance in the relative gene expression compared to untreated cells, at 24 h; # $p < 0.05$ and ## $p < 0.01$ represent the difference significance in the relative gene expression between samples treated for 6 h *versus* those treated for 24 h).

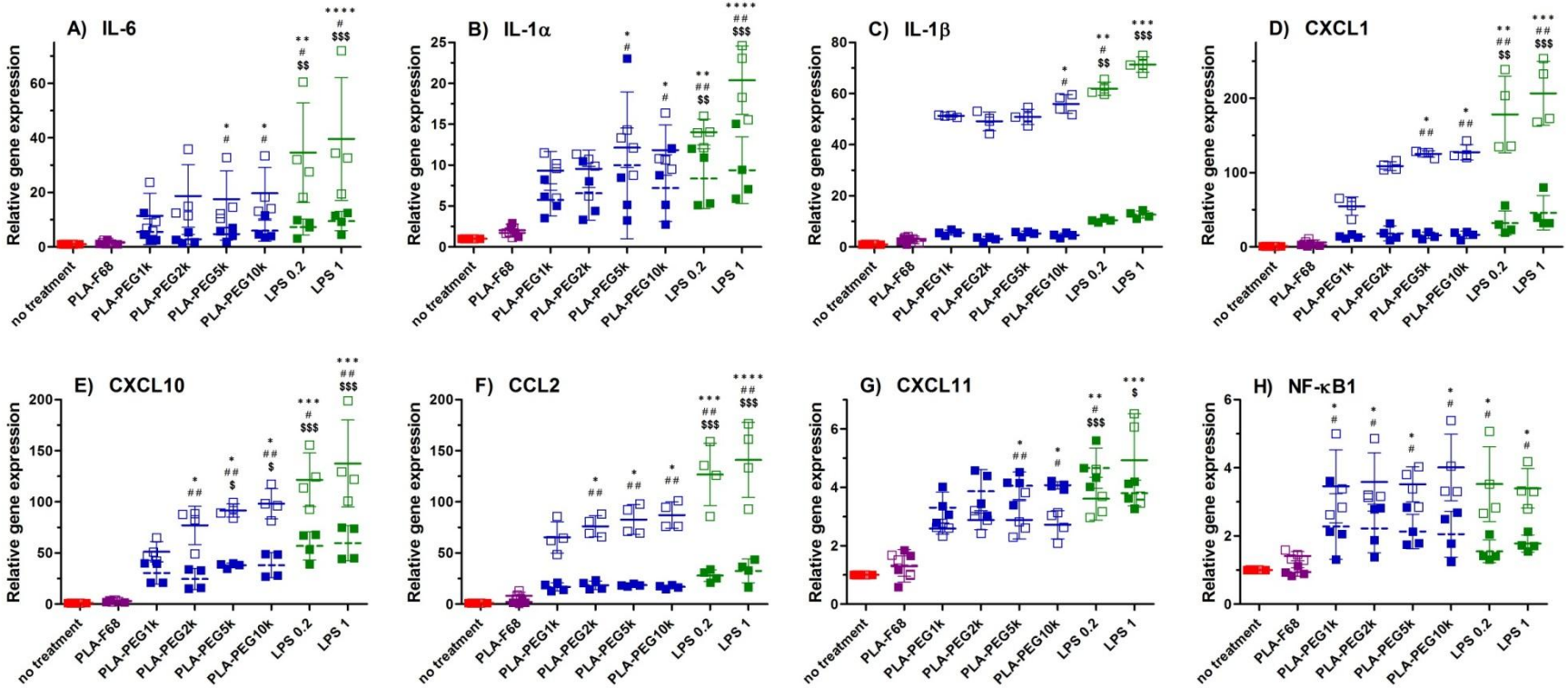

Figure 4. Relative mRNA expression for inflammatory cytokines and chemokines in HUVEC. A) IL-6, B) IL-1α, C) IL-1β, D) CXCL1, E) CXCL10, F) CCL2, G) CXCL11 and H) NF-κB1, in HUVEC treated with PLA-F68 (□/■) and PLA-PEGX NPs (X from 1 to 10 kDa) (□/■) for 6 (□/□/□/□) and 24 h (■/■/■/■), at 1,000 µg/mL, *versus* untreated cells (□/■). Two LPS concentrations (0.2 and 1 µg/mL) were used as positive controls (□/■) (n = 4 independent samples; mean ± SD; * $p < 0.05$, ** $p < 0.01$, *** $p < 0.001$ and **** $p < 0.0001$ represent the difference significance in the relative gene expression compared to untreated cells, at 6 h; $ $p < 0.05$, $$ $p < 0.01$ and $$$ $p < 0.001$ represent the difference significance in the relative gene expression compared to untreated cells, at 24 h; # $p < 0.05$ and ## $p < 0.01$ represent the difference significance in the relative gene expression between samples treated for 6 h *versus* those treated for 24 h).

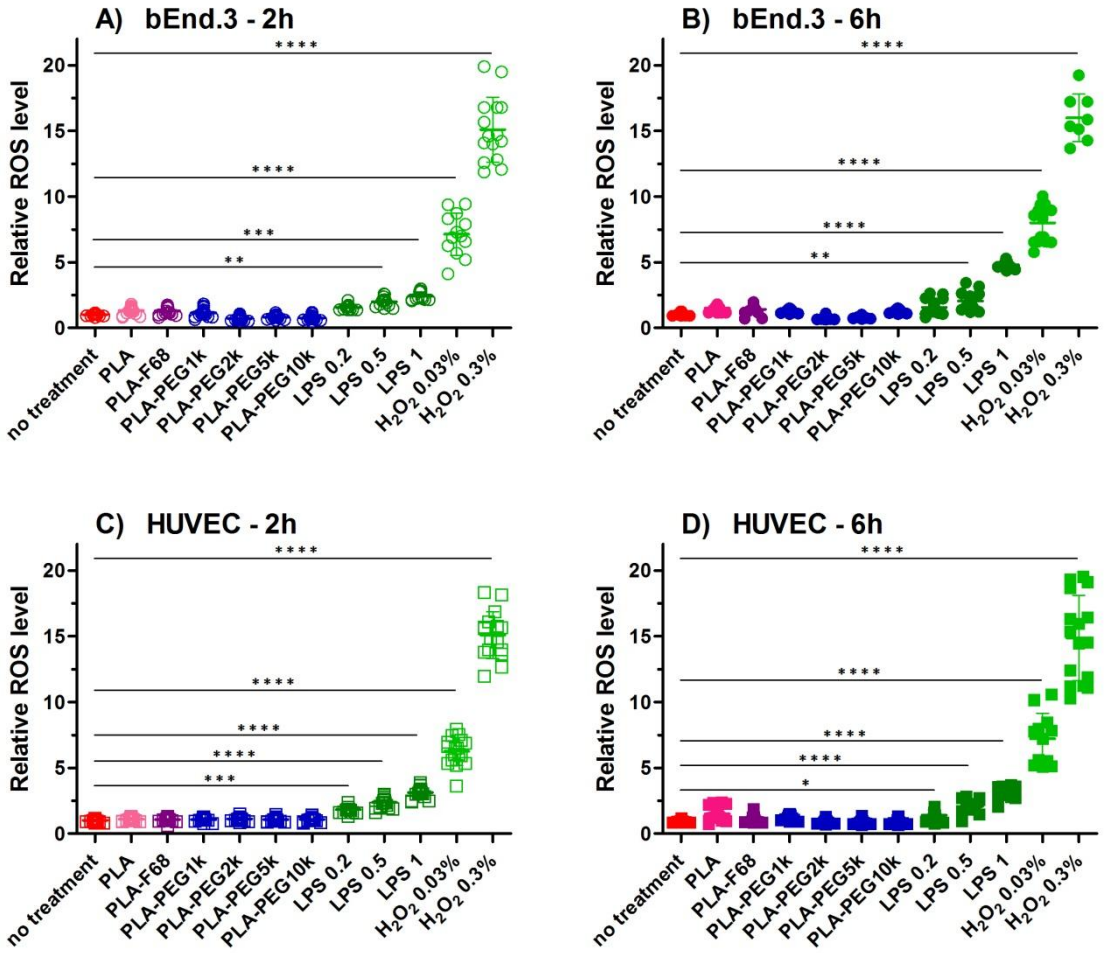

Figure 5. Oxidative stress response in vascular endothelial cells. Oxidative stress response after treating bEnd.3 cells (A/B) and HUVEC (C/D) with PLA (○/●/□/■), PLA-F68 (○/●/□/■) and PLA-PEGX NPs (X from 1 to 10 kDa) (○/●/□/■) for either 2 (A/C) or 6 h (B/D), at 1,000 µg/mL. Untreated cells were used as negative controls (○/●/□/■) and 3 LPS concentrations (0.2, 0.5 and 1 µg/mL) (○/●/□/■) and 2 H_2O_2 concentrations (0.03 and 0.3 % (*v/v*)) (○/●/□/■) were used as positive controls (n = 4 independent assays and quadruplicate wells per sample per assay; mean ± SD; * p < 0.05, ** p < 0.01, *** p < 0.001 and **** p < 0.0001 represent the difference significance in the oxidative stress response compared to untreated cells).